J. Biochem. 2010;147(5):679–688 doi:10.1093/jb/mvp212

JB THE JOURNAL OF BIOCHEMISTRY

Purification and characterization of new phytoferritin from black bean (*Phaseolus vulgaris* L.) seed

Received November 25, 2009; accepted December 20, 2009; published online January 6, 2010

Jianjun Deng[1], Xiayun Liao[1], Ju Hu[1], Xiaojing Leng[1], Jianjun Cheng[2] and Guanghua Zhao[1,*]

[1]CAU and ACC Joint-Laboratory of Space Food, College of Food Science and Nutritional Engineering, China Agricultural University, Beijing 100083 and [2]The Key Laboratory of Soybean Biology of Education Ministry, Food Science College, Northeast Agricultural University, Harbin 150030, People's Republic of China

*Guanghua Zhao, College of Food Science and Nutritional Engineering, China Agricultural University, Beijing 100083, People's Republic of China. Tel: +86-10-62737761, Fax: +86-10-62737761, email: gzhao1000@yahoo.com

In contrast to animal ferritin, relatively little information is available on phytoferritin. Black bean (*Phaseolus vulgaris* L.) has been consumed in many countries. In the present study, new ferritin from black bean seed was purified by two consecutive anion exchange and size exclusion chromatography. The apparent molecular mass of the native black bean seed ferritin (BSF) was found to be ~560 kDa by native PAGE analysis. N-terminal sequence, MALDI-TOF-MS and MS/MS analyses indicate that BSF and soybean seed ferritin (SSF) share very high identity in amino acid sequence. However, SDS–PAGE result indicates that BSF consists of 26.5 (H-1) and 28.0 kDa (H-2) subunits with a ratio of 2 : 1, while the ratio of these two subunits in SSF is 1 : 1. This result demonstrates that the two proteins have different subunit composition which might affect their activities in iron uptake and release. Indeed, at high iron flux, the initial rate of iron oxidative deposition in apoBSF is larger than that in apoSSF. On the contrary, the iron release from BSF is significantly slower than that from SSF. All these results indicate that phytoferritin might regulate the transit of iron into and out of the protein cavity by changing its subunit composition.

Keywords: black bean/ferritin/iron oxidative deposition/iron release/MALDI-TOF-MS.

Abbreviations: ACN, acetonitrile; BSF, black bean seed ferritin; CHCA, α-cyano-4-hydroxy cinnamic acid; EP, extension peptide; GFC, gel filtration chromatography; IEC, ion exchange chromatography; MALDI, matrix-assisted laser desorption ionization; Mops, 3-(N-morpholino)propanesulfonic acid; PMF, peptide mass fingerprint; PSF, pea seed ferritin; PVP, polyvinylpyrrolidone; SDS, sodium dodecyl sulfate; SSF, soybean seed ferritin; TFA, trifluoroacetic acid; TOF, time of flight; TP, transient peptide; Tris, tris(hydroxymethyl)aminomethane.

Iron is an element essential for all forms of life because of its role in major biological processes such as the tricarboxylic acid cycle, electron transport, nitrogen fixation, DNA synthesis and detoxication reaction (*1*). Ferritins are a broad superfamily of iron storage proteins, found in a wide range of animals, plants, fungi and bacteria, except in yeast. It could either sequester excess iron taken up by the cell or release stored iron to meet the cell's metabolic needs during iron scarcity (*2*, *3*). It is composed of 24 subunits arranged in 432 symmetry to form a hollow protein shell (outside diameter is 12–13 nm, inside 7–8 nm), capable of storing a maximum of ~4,500 Fe^{3+} atoms in the central cavity as a hydrous ferric oxide (*2*). In vertebrates, ferritins consist of two types of subunit: H (heavy) and L (light), with apparent molecular weights of 21 and 19.5 kDa, respectively (*4*). The two have ~55% identity in amino acid sequence. The H-subunit contains a dinuclear ferroxidase centre necessary for iron uptake and oxidation of ferrous iron, and consists of A and B iron binding sites of conserved amino acid ligands Glu27, His65, Glu62 and Glu107. H-bonding residues Gln141 and Tyr34 are nearby the B-site (*5*, *6*). In contrast, the L-subunit lacks a ferroxidase centre but contains a putative nucleation site important for slower iron oxidation and mineralization (*7*). The shape of the subunit is cylindrical, with a length of 5 nm and width of 2.5 nm. Each subunit is composed of a four-α-helix bundle containing two antiparallel helix pairs (A, B and C, D) and a fifth short helix (helix E). The E helix lies at one end of the bundle at ~60° to its axis and forms a hydrophobic pore (*2*, *3*, *8*).

Sequence comparison of plant and animal ferritins demonstrates that both of them have evolved from a common ancestor (*9*). However, phytoferritin exhibits various specific features as compared to animal ferritins: phytoferritin is observed in plastids (chloroplasts in leaves, amyloplasts in tubers and seeds, etc.), whereas animal ferritins are located in the cytoplasm of cell (*2*, *10*). The expressions of animal ferritins are strictly regulated via the interaction between iron responsive elements (IREs) and iron regulatory proteins (IRPs) at the translational level (*11*), but the expression of phytoferritin genes are controlled at the transcriptional level (*12*). Different from animal ferritins, only one type of subunit has been identified in phytoferritin, which shares ~40% sequence identity with the animal H-subunit (*12*, *13*). Ferritin from soybean and pea seed consists of two subunits of 26.5 and 28.0 kDa, which are designated H-1 and H-2,

respectively, sharing ~80% amino acid sequence identity (*13*, *14*). The two subunits are synthesized as a precursor (32 kDa) with a unique two-domain N-terminal sequence, the transit peptide (TP) that is followed by an extension peptide (EP). The TP is presumed to facilitate transport of the ferritin precursor to plastids (*15*). Upon transport to plastids, the TP is cleaved from the subunit precursor, resulting in the formation of the mature subunit which assembles into a 24-mer apoferritin within the plastids (*10*). The EP is a part of the mature phytoferritin. Recent studies from our group revealed the functional role for the EP during iron oxidative deposition in phytoferritin as a second binding and ferroxidase centre that contributes to mineralization of the iron core at high iron loadings of ferritin (>48 iron/protein shell) (*16*). In addition, it suggests that it could be involved in the loss of protein solubility and stability during iron-exchange *in vitro* (*17*) and *in vivo* during the early steps of germination (*18*).

To date, animal and bacterial ferritins have received great attentions (*1–3*). In contrast, relatively little is known about phytoferritin. Black bean, as a healthy food and herbal material, has been cultivated and consumed in many countries throughout the world and have both economic and nutritional importance. Besides a plentiful supply of protein and calories, a lot of the micronutrients are present in black bean, such as anthocyanins, vitamin E, isoflavones, saponins and carotenoids, which have been reported to exert biological activity (*19*). In this article, new phytoferritin from black bean seed was purified and characterized by gel electrophoresis, MALDI-TOF mass spectroscopy and N-terminal sequence determination. Since black bean and soybean belong to the same genus, we compared iron uptake and release activities between black bean seed ferrittin (BSF) and soybean seed ferritin (SSF) to understand the relationship of structure and function of phytoferritin.

Materials and Methods

Materials

Dried black bean and soybean seeds were obtained from the local market. 3-(N-morpholino) propanesulfonic acid (Mops) and polyvinylpyrrolidone (PVP) were obtained from Amresco (USA). Ascorbate, sodium citrate and magnesium chloride hexahydrate were purchased from Beijing chemical reagents Co. (Beijing, PR China). Ferrous sulphate, sodium dithionite, 2,2′-bipyridyl,N′, N′-*bis*-methyleneacrylamide, sodium dodecyl sulphate (SDS), tris(hydroxymethyl)aminomethane (Tris), TEMED, β-mercaptoethanol, coomassie brilliant blue R250 and the ferrous iron chelator 3-(2-pyridyl)-5,6-bis(4-phenyl-sulfonic acid)-1,2,4-triazine (ferrozine) were obtained from Sigma-Aldrich Co. (Beijing, PR China). All other reagents used were of analytical grade or purer.

Protein isolation and purification

Approximately 1 kg of black bean seeds was soaked in distilled water overnight, decorticated and blended in three volumes of extraction buffer (50 mM KH_2PO_4–Na_2HPO_4, pH 7.0, 1% PVP), filtered through cheesecloth and the residue was removed. The filtrate was incubated for 10 min at 50°C, and then centrifuged at 16,500×*g* for 10 min to separate the insoluble material. The supernatant was adjusted to 300 mM $MgCl_2$, stored for 30 min at 4°C. It was followed by addition of sodium citrate to final concentration of 450 mM to complex the magnesium. After 8 h, this supernatant was centrifuged at 23,800*g* for 40 min at 4°C. The brown pellet thus obtained was dissolved in 50 mM KH_2PO_4–Na_2HPO_4 buffer (pH 7.5), and was dialysed against the same buffer three times. The protein was further purified by ion exchange chromatography (IEC) in a DEAE-Sepharose Fast Flow column previously equilibrated in 50 mM KH_2PO_4–Na_2HPO_4 buffer (pH 7.5). Fractions containing BSF were pooled and concentrated, and finally loaded to Sephacryl S-300 gel filtration chromatography (GFC) equilibrated before use in 50 mM KH_2PO_4–Na_2HPO_4 buffer (pH 7.5, 0.15 M NaCl). Ferritin from soybean seeds was prepared as previously described (*13*). Native PAGE and SDS–PAGE analyses of purified SSF were shown in Supplementary Fig. S1.

Apoferritin preparation

Apoferritin was prepared according to reported methods with some modifications (*20*, *21*). The protein was rendered iron free by anaerobic reduction with 55 mM sodium dithionite in 50 mM Tris–HCl, pH 7.5 for 6 days followed by 2 days anaerobic dialysis of the protein against 1 mM 2,2′-dipyridyl, 5 mM Mops (pH 7.9) to chelate the Fe^{2+} produced during the reduction. The resulting solution was then dialysed against 5 mM Mops (pH 7.9), and finally against the working buffers indicated in the figure captions. The protein concentration was determined by the Lowry method with BSA as standard (*22*). Holoferritins with different sizes of iron core were prepared as previously described (*23*). Briefly, different increments (*1–17*) of 1 µl of 48 mM $FeSO_4$ in ddH_2O, pH 2, were added to apoBSF and apoSSF (1.0 µM) at intervals of at least 30 min over a period of 2 days to give different iron loadings from 48 to 800 Fe^{3+}/protein, respectively.

Polyacrylamide gel electrophoresis

The molecular weight of the native BSF was estimated by PAGE using a 4–20% polyacrylamide gradient gel run at 25 V for 14 h at 4°C employing Tris–HCl (25 mM, pH 8.3) as running buffer. Gels were stained with Coomassie brilliant blue R250. Gel electrophoresis under denaturing conditions was carried out with 15% polyacrylamide–SDS gel as reported by Laemmli (*24*). Protein samples (~20 µg) were suspended in 50 µl of water. To the solution were added 100 µl of sample buffer containing 25% glycerol, 12.5% 0.5 M Tris–HCl, pH 6.8, 2% SDS, 1% bromophenol blue and 5% β-mercaptoethanol. After the solution was boiled for 10 min, the supernatant was isolated by centrifugation at 10,000*g* for 10 min.

In-gel trypsin digestion

BSF and SSF subunits (28.0 and 26.5 kDa) were separated electrophoretically using a 15% SDS–polyacrylamide gel (SDS–PAGE). Their gel bands, ~1 mm^2, were excised from the gel with a pipette tip and transferred to 1.5 ml microtubes. To each tube, 100 µl of destaining solution of 50 mM NH_4HCO_3 in 50% acetonitrile (ACN) were added and the mixture was incubated for 20 min. The solution was discarded and this process was repeated three times or until the blue color of the gel piece was completely removed. Then 200 µl of 100% ACN were added and incubated for 10 min. The gel piece changed from semi-transparent to opaque white. The solution was removed and the gel pieces were dried in a SpeedVac for 15 min. After that, 5 µl of trypsin solution (0.005 µg $µl^{-1}$ in 25 mM NH_4HCO_3, pH 8.0) were added to each tube and incubated at 37°C overnight. The peptides were recovered from the gel pieces by incubating with 50 µl of extraction solution of 50% ACN/0.1% trifluoroacetic acid (TFA) for 30 min. The extracted peptide solution was dried in the SpeedVac to ~10 µl and stored at −20°C for future use. Peptides were desalted and concentrated using Ziptip C-18 columns before MS analysis (*14*).

Peptide mass fingerprinting (PMF) by MALDI-TOF-MS and peptide sequencing by MALDI-TOF-MS/MS

All mass spectra of MALDI-TOF-MS and MALDI-TOF-MS/MS were obtained on a Bruker ultraflex III TOF/TOF (Bruker Daltonik GmbH, Germany) in positive ion mode at an accelerating voltage of 20 kV with a nitrogen laser (337 nm). The spectra were internally calibrated using trypsin autolysis products. The ferritin peptide sample was desalted with a spin column (Pierce) before MALDI-TOF-MS analysis. Approximately 0.5 µl of sample and 0.5 µl of matrix were spotted onto a stainless steel target plate and allowed to air-dry before analysis. The samples were ablated using ~100 laser shots fired in 10 shot packets while the laser rastered over the target surface (*14*). All of the spectra were acquired in the

positive ion reflection mode using α-cyano-4-hydroxy cinnamic acid (CHCA) (10 mg ml^{-1} in 50% ACN/0.1% TFA) as the matrix. PMFs obtained were used to search through the SWISS-PROT and NCBInr database by the MASCOT search engine (http://www.matrixscience.com) with one missed cleavage site. The amino acid sequences of the peptides were deduced with the peptide-sequencing program MasSeq. The database search was finished with the Mascot search engine (http://www.matrixscience.com) using the data processed through MaxEnt3 and MasSeq.

N-Terminal amino acid sequence

The amino acid sequence of the N-terminus was determined on a protein sequencer (Applied Biosystems Procise-PROCISE 491) using automated Edman degradation. After SDS–PAGE, protein was transferred to a polyvinylidene difluoride membrane (Millipore) and stained with Coomassie brilliant blue R250. The two subunits were eluted from the membrane, and the sequences of the 15 amino acids at the N-terminus were determined for each subunit.

Fe^{2+} oxidative deposition in ferritin

The fast kinetic experiments were undertaken with the pneumatic drive Hi-Tech SFA-20M stopped flow accessory on a Varian Cary 50 spectrophotometer (Varian, USA). Equal 140 µl volumes of a weakly acidic $FeSO_4$ solution (48 or 200 µM) and buffered apoferritin solution (1.0 µM) were mixed at 25°C in the thermostatted sample compartment containing a 280 µl quartz stopped flow cuvette with 1 cm optical path length. All quoted concentrations are final concentrations after mixing the two reagents together. µ-oxo diFe^{3+} species formed during Fe^{2+} oxidation were monitored by 300 nm. Data were acquired every 12.5 ms (the shortest acquisition time possible with the Cary 50). The spectrophotometer was operated in single beam mode and zeroed prior to each kinetic run with a cuvette containing apoferritin in buffer. The kinetic data was curve fitted with Origin 7.5 software (Micro Cal Inc.). The initial rate (v_0) of iron oxidation measured as µ-oxo complex formation was obtained as previously described (*25*).

Kinetic measurement of iron release

Iron release from holoferritin was investigated by using the assay procedure previously described (*26*). Typically, the assay system (total volume 1 ml) contained 0.2 µM ferritin, 500 µM ferrozine, 0.15 M NaCl, 1 mM ascorbate and 50 mM Mops buffer, pH 7.0. Reactions were carried out at 25°C against reference cuvettes containing all reactants and were initiated by the addition ascorbate. The development of $[Fe(ferrozine)_3]^{2+}$ was measured by recording the increase in absorbance at 562 nm using a Varian Cary 50 spectrophotometer and iron released was estimated using $\varepsilon_{562} = 27.9\ mM^{-1}\ cm^{-1}$. The kinetic data were further analysed with Origin 7.5 software (Micro Cal Inc.). The initial rate (v_0) of iron release measured as Fe^{2+}-ferrozine complex formation was obtained as previously reported (*25*).

Results and discussion

Purification of BSF

BSF was extracted from dry seeds and purified using the following sequential purification steps: salting out with $MgCl_2$ and sodium citrate, IEC on a DEAE-Sepharose Fast Flow column, and GFC on a Sephacryl S-300 column. A heating procedure was used for the ferritin purification prior to above three steps, namely, black bean seed slurry was kept at 50°C for 10 min to denature proteases and other heat sensitive proteins. After IEC was eluted with a linear gradient of NaCl (0–0.8 M) in the phosphate buffer at a flow rate of 1.0 ml min^{-1}, two main peaks were collected as shown in Fig. 1. Since peak 1 contained more amounts of iron than peak 2, the fraction corresponding to peak 1 was subjected to GFC in the phosphate buffer at a flow rate of 0.4 ml min^{-1}, with a typical elution profile revealing one peak of 280 nm absorbing material (Fig. 2). Non-denaturing gel electrophoresis (native PAGE) resolved purified BSF as a single complex with an apparent molecular weight estimated to be ~560 kDa (Fig. 3A). SDS–PAGE was run to analyse the composition of ferritin subunits, and was displayed in Fig. 3B. While purified ferritin subunits are composed of 28.0 and 26.5 kDa (Fig. 3B), densitometric analysis shows that the two subunits are present in native BSF is an ~1 : 2 ratio of 28.0 versus 26.5 kDa subunit (Fig. 3B). Thus, the subunit composition of BSF is distinct from those of pea seed ferritin (PSF) and SSF where the ratio of 28.0 kDa subunit to 26.5 kDa subunit is 2:1 (*26*) and 1 : 1 (*13*), respectively. These results indicate that BSF is different from its analogues in structure. According to above procedures, ~20–30 mg of ferritin were yielded from 1 kg of dry black bean seeds. This yield is about a half of

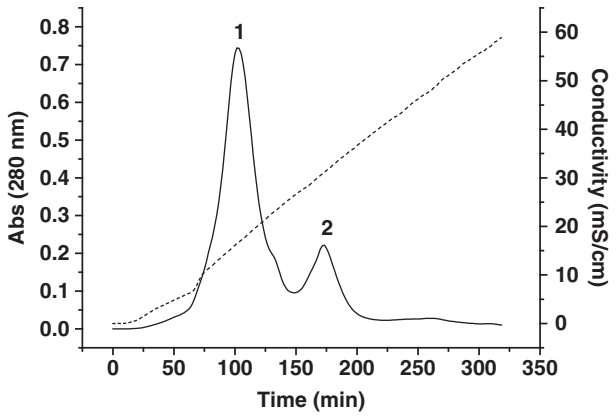

Fig. 1 Elution profile of chromatography of BSF on DEAE-Sepharose Fast Flow column. Crude protein sample (30 ml) was subjected to an anion exchange column pre-equilibrated with 50 mM KH_2PO_4–Na_2HPO_4 buffer (pH 7.5). Column was eluted with a linear gradient of NaCl (0–0.8 M) in the phosphate buffer at a flow rate of 1.0 ml min^{-1}. The volume of each fraction was 5 ml. Protein was monitored by measuring absorbance at 280 nm.

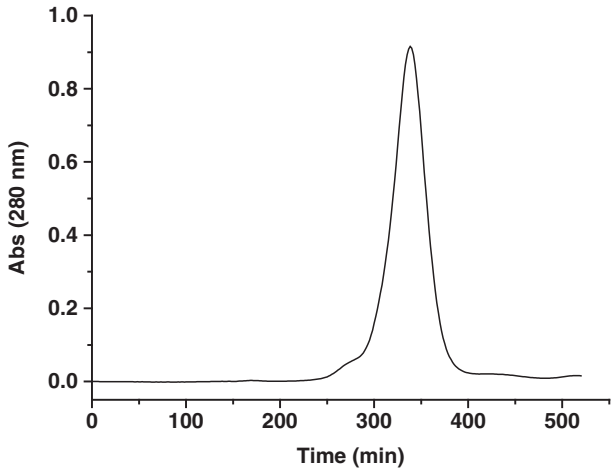

Fig. 2 Elution profile of chromatography of BSF on Sephacryl S-300 gel filtration column. The column was equilibrated with 50 mM KH_2PO_4–Na_2HPO_4 buffer (pH 7.5) containing 0.15 M NaCl. The column was eluted with the same buffer at a flow rate of 0.4 ml min^{-1}. The volume of each fraction was 5 ml. Protein was monitored by measuring absorbance at 280 nm.

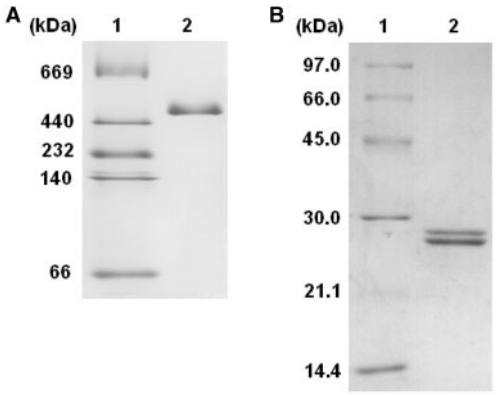

Fig. 3 Native PAGE and SDS–PAGE analyses of purified ferritin from black bean seed. Sample was loaded after the final gel filtration chromatography on Sephacryl S-300 column. (A) native PAGE, (B) SDS–PAGE. Lane 1, protein markers and their corresponding molecular masses; Lane 2, BSF.

that for phytoferritin from soybean seed (*27*). The protein as isolated contains ~1,200–1,800 g atoms of iron per mol of protein.

Comparison of PMFs of BSF with those of SSF

The PMFs of the SDS–PAGE gel bands of 28.0 and 26.5 kDa of BSF were acquired by MALDI-TOF mass spectrometry using CHCA as the matrix. Since black bean and soybean originate from the same genus, we also obtained the PMFs from SSF to determine whether there is a difference in PMF between BSF and SSF. The MALDI-TOF-MS spectra of the gel band 28.0 and 26.5 kDa of both BSF and SSF generated from in-gel trypsin digestion are shown in Fig. 4. There are four abundant peptide ions of m/z 1,238; 1,638; 1,766 and 2,236 in the tryptic PMF of the 28.0 kDa of both BSF and SSF except that one ion

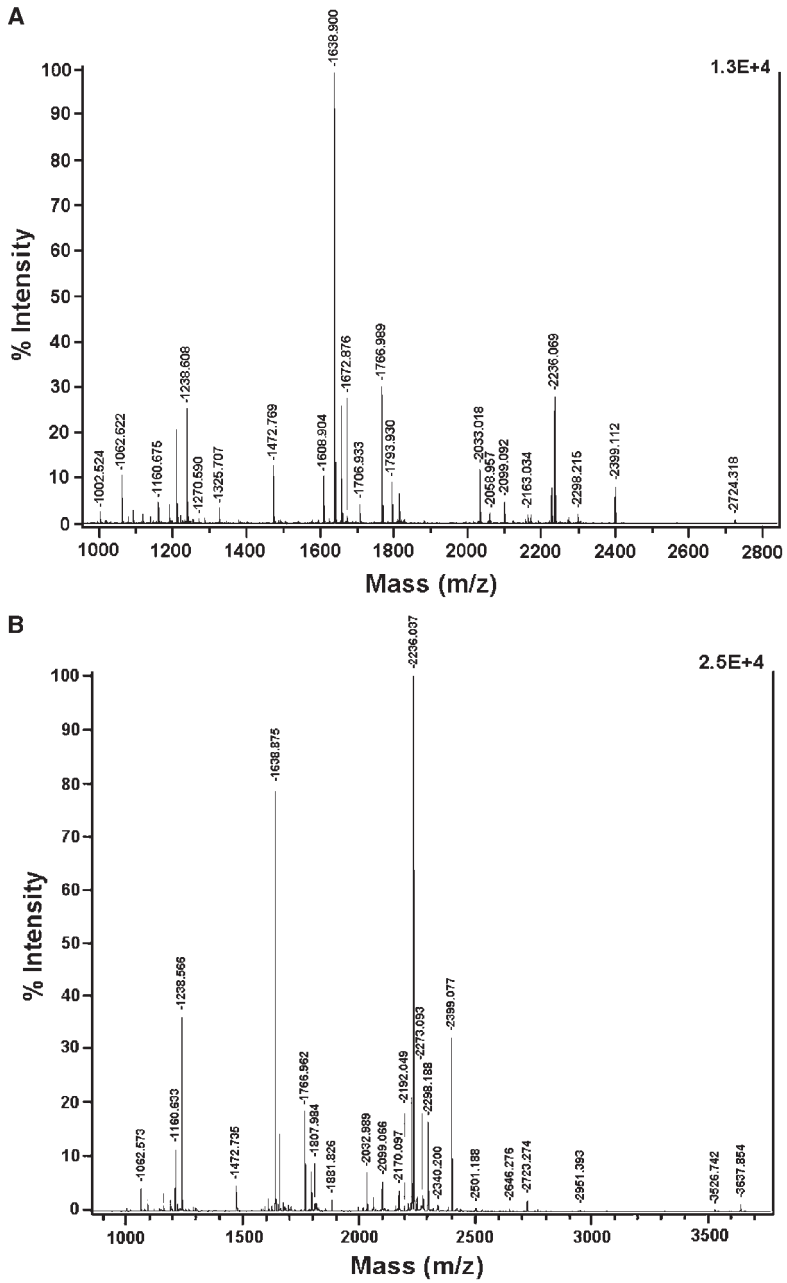

Fig. 4 Tryptic PMF of the 28.0 kDa gel bands of BSF (A) and SSF (B) from SDS–PAGE acquired by MALDI-TOF-MS.

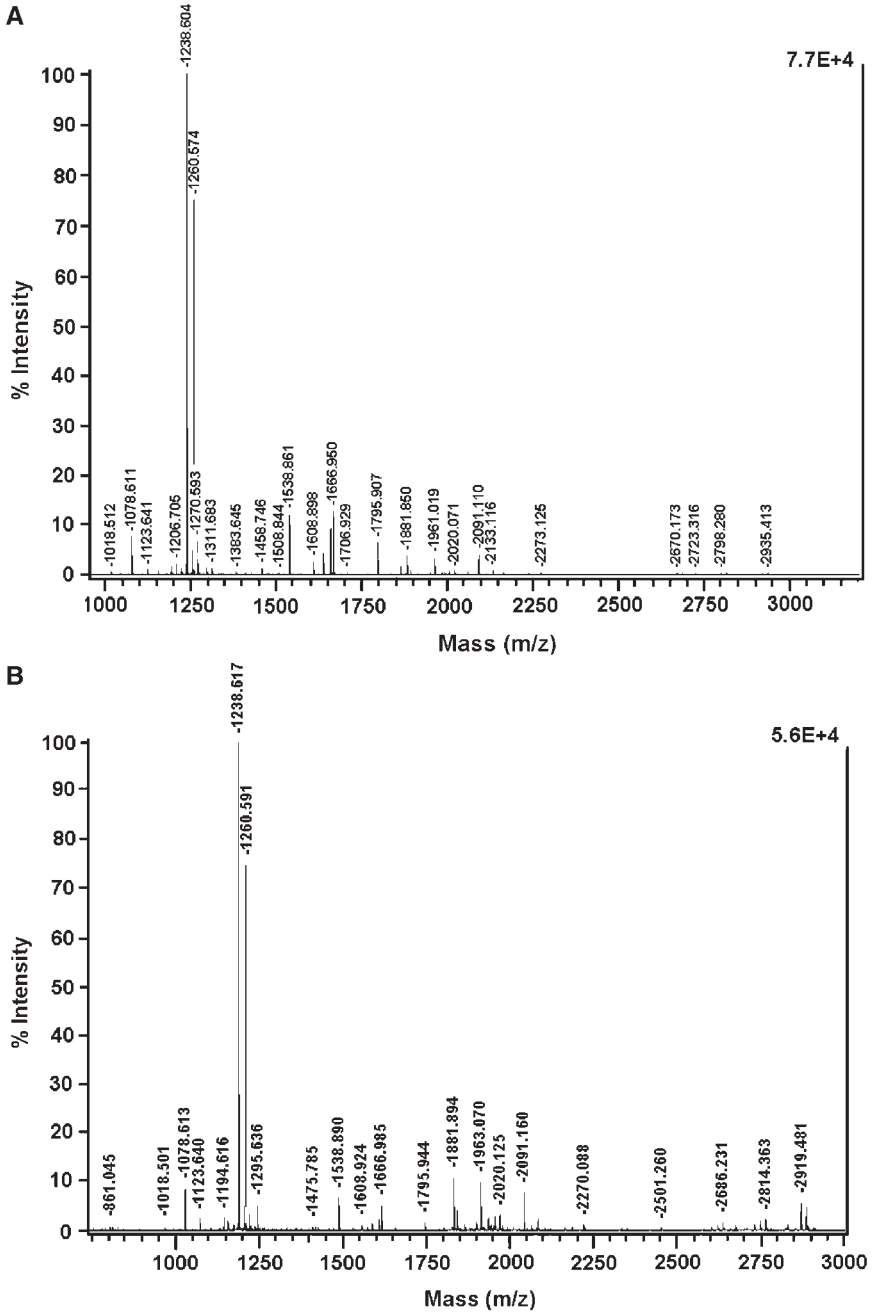

Fig. 5 Tryptic PMF of the 26.5 kDa gel bands of BSF (A) and SSF (B) from SDS–PAGE acquired by MALDI-TOF-MS.

at *m*/*z* 1672 only appears in the PMF of the 28.0 kDa of BSF, indicating that their 28.0 kDa subunits share high identity in the amino acid sequence. Likewise, we compared the PMF of the 26.5 kDa gel band of BSF and SSF, and the results were given in Fig. 5. Generally, their PMFs were nearly identical with each other. For example, two predominant MALDI-TOF peaks at *m*/*z* 1,238 and 1,260 appear in their PMF with nearly the same intensity. Similar features are observed with other relatively weak peaks containing *m*/*z* 1,018; 1,078; 1,123; 1,538; 1,666; 1,795; 2,091 and so on. This result suggests that the amino acid sequence of the 26.5 kDa subunits of BSF and SSF shares higher homology than that of their 28.0 kDa subunits.

Furthermore, the peptide mass data of the gel bands of 28.0 and 26.5 kDa, respectively, as listed in Tables I and II, were searched in the protein database NCBInr 20081101 that contains 7,241,274 sequences entries using the MASCOT search program (http://www.matrixscience.com). The search parameters are summarized in Table III. Protein scores >70 are considered significant ($P < 0.05$). It is found that the PMF of both 26.5 and 28.0 kDa subunits from BSF matched significantly to that of the ferritin subunits from the soybean, the probability-based Mowse score of the 28.0 kDa subunit (104) is markedly lower than that of the 26.5 kDa analogue (*362*), a result being consistent with the above idea that the amino acid sequence of the 26.5 kDa subunits of BSF and SSF shares higher

Table I. Mass peaks of gel bands 28 kDa for MASCOT database search.

Gel band 28 kDa of BSF PMF (m/z)		Gel band 28 kDa of SSF PMF (m/z)	
1,002.524	1,813.852	1,002.471	2,099.066
1,020.506	2,033.018	1,062.573	2,156.112
1,062.622	2,058.957	1,092.577	2,170.097
1,078.616	2,099.092	1,139.549	2,192.049
1,092.630	2,163.034	1,160.633	2,210.012
1,139.593	2,170.117	1,190.672	2,221.054
1,160.675	2,227.117	1,194.553	2,227.155
1,190.711	2,236.069	1,210.558	2,236.037
1,210.600	2,273.133	1,220.677	2,252.031
1,220.726	2,298.215	1,238.566	2,268.152
1,238.608	2,399.112	1,472.735	2,273.093
1,242.597	2,724.318	1,608.865	2,277.060
1,270.590		1,638.875	2,293.055
1,287.608		1,656.853	2,298.188
1,325.707		1,672.849	2,340.200
1,472.769		1,766.962	2,399.077
1,608.904		1,793.904	2,421.048
1,623.859		1,807.984	2,501.188
1,638.900		1,809.885	2,646.276
1,656.880		1,881.826	2,723.274
1,672.876		1,993.929	2,768.303
1,706.933		2,014.969	2,951.393
1,766.989		2,032.989	3,526.742
1,793.930		2,058.929	3,637.854

Table II. Mass peaks of gel bands 26.5 kDa for MASCOT database search.

Gel band 26.5 kDa of BSF PMF (m/z)		Gel band 26.5 kDa of SSF PMF (m/z)	
1,018.512	1,636.935	855.037	1,949.052
1,044.518	1,638.870	861.045	1,963.071
1,078.611	1,658.855	877.042	1,985.054
1,123.641	1,666.950	1,018.501	1,991.049
1,155.575	1,706.929	1,078.613	1,993.995
1,192.589	1,795.907	1,123.640	2,001.017
1,194.612	1,863.022	1,192.608	2,005.079
1,206.705	1,881.850	1,194.616	2,020.125
1,221.570	1,891.983	1,206.717	2,027.055
1,223.579	1,948.996	1,223.697	2,091.160
1,223.792	1,963.019	1,238.617	2,113.140
1,238.604	1,985.000	1,254.613	2,133.169
1,243.588	1,991.006	1,260.591	2,236.103
1,254.595	2,005.027	1,270.602	2,270.088
1,260.574	2,020.071	1,276.568	2,501.260
1,270.593	2,058.962	1,287.616	2,652.264
1,276.554	2,091.110	1,295.636	2,670.2302
1,287.600	2,113.068	1,458.722	2,686.231
1,295.621	2,133.116	1,475.785	2,723.361
1,300.520	2,163.018	1,538.890	2,780.367
1,311.683	2,236.056	1,608.924	2,798.336
1,314.637	2,270.045	1,623.852	2,814.336
1,383.645	2,273.125	1,636.968	2,879.755
1,409.618	2,670.173	1,638.905	2,919.481
1,425.608	2,686.170	1,658.888	2,935.476
1,458.746	2,723.316	1,666.985	2,941.459
1,475.763	2,798.280	1,795.944	2,957.444
1,508.844	2,814.276	1,881.894	
1,538.861	2,919.413	1,892.032	
1,608.898	2,935.413	1,914.015	

identity than that of their 28.0 kDa ones. The complete amino acid sequence of SSF is shown in Fig. 6A (*13*). Sequence comparisons between the peptides from the MASCOT program and those from the reported

Table III. MASCOT search parameters for the gel bands 28.0 and 26.5 kDa.

Type of search	Peptide mass fingerprint
Enzyme	Trypsin
Mass values	Monoisotopic peak
Protein mass	28.0 or 26.5 kDa
Peptide mass tolerance	±0.3 Da
Fragment mass tolerance	±0.5 Da
Max missed cleavages	2
Number of queries	36 for 28.0 kDa; 60 for 26.5 kDa

amino acid sequence of SSF revealed that five amino acids including Ile-73, Leu-78, Thr-141, Ala-180 and Lys-201 may be replaced by Val, Phe, Val, Ser and Arg, respectively (Fig. 6A, in blue). In contrast, only one amino acid was detected with difference from that of the 26.5 kDa subunit in SSF where the alanine was replaced by the valine at position 113 (Fig. 6A, in blue). This result further confirms the above conclusion.

To seek more evidence for the above conclusion, peptide sequences of the PMF with the 26.5 and 28 kDa subunits in BSF, were analysed by MALDI-TOF-MS/MS (Supplementary Figs. S2 and S3). The stronger PMF peaks m/z 1,638 and 1,238 from gel bands 28.0 and 26.5 kDa, respectively, from both BSF and SSF were found to have amino acid sequences RALSVNHAIPVALYD and RQDFHWVGHG (Fig. 6A, underlined). The latter sequence corresponds to the last positions from 4 to 13 at the C-terminal of the 26.5 kDa subunit (Fig. 6A). Thus, in mature BSF and SSF, their C-terminals possibly remain intact. This result conflicts with previous hypothesis that the initial 26.5 kDa also occurs in its 28.0 kDa form, but the 28 kDa subunit is unstable and could be readily converted to 26.5 kDa by cleavage of the 16 residues at the C-terminus (*13*). Consistent with the present observation, the same ion peak at ~1,238 representing amino acid sequence RQDFHWVGHG likewise appears in the 26.5-kDa subunit of mature PSF (*14*). However, it is likely that the C-terminal of the 26.5 kDa is partially degraded.

Moreover, the PMF peaks m/z 1,766 and 2,236 from gel band 28.0 kDa with BSF were also analysed by MALDI-TOF-MS/MS (Supplementary Fig. S2) and had amino acid sequences RALSVNHAIPVALYDK and KILQEAHEREEESSEKFF (underlined), respectively, which perfectly matched the corresponding H-2 amino acid sequences of SSF (Fig. 6A) (*13*). Meanwhile, the peaks m/z 1,078; 1,538 and 1,666 from gel band 26.5 kDa with BSF were also analysed, respectively, by MALDI-TOF-MS/MS (Supplementary Fig. S3) and had amino acid sequences RLQAVYESI, RALSVQPATPVALES and RALSVQPATPVALESK (underlined), which perfectly matched to the corresponding H-1 amino acid sequences of reported SSF (Fig. 6A) (*13*). It was also found that the amino acids of ferroxidase centre in BSF matched significantly those in SSF (Fig. 6A). Finally, the 15 N-terminal sequence residues of two

A

28.0 kDa

1 **ASNAPAPLAGVIFEP**FQELKKDYLAVPIAHNVSLARQNYADDSESAINEQ
KDYLAVPIAHNVSLAR
51 INVEYNVSYVYHAL FAYFDRDN**I**ALKG **L**AKFFKESSEEEREHAEQLIKYQ
DN**V**ALKG**F**AKFFKESSEEEREHAEQLIK
101 NIRGGRVVLHPITSPPSEFEHSEKGDALYAMELALSLEKL**T**NEKLLHVHS
GDALYAMELALSLEKL**V**NEKLLNVHS
151 VADRNNDPQLADFIESEFLYEQVKSIKKI**A**EYVAQLRLVGKGHGVWHFDQ
VADR **I**SEYVAQLR GHGVWHFDQ
201 **K**LLHDEDHV
R

26.5 kDa

1 **ASTVP--LTGVIFEPFE**EVKKSELAVPTAPQVSLARQNYADECESAINEQIN
KSELAVPTAPQVSLAR
51 VEYNASYVYHSLFAYFDRDNVALKGFAKFFKESSEEEREHAEKLMKYQ
FFKESSEEEREHAEK
99 NTRGGRVVLHPIKN**A**PSEFEHVEKGDALYAMELALSLEKLVNEKLLNVHS
N**V**PSEFEHVEKGDALYAMELALSLEKLVNEKLLNVHS
149 VADRNNDPQMADFIESEFLSEQVESIKKISEYVAQLRRVGKGHGVWHFDQ
VADRNNDPQMADFIESEFLSEQVESIKKISEYVAQLR GHGVWHFDQ
199 RLLD
R

B

28.0 kDa ASNAPAPLAGVIFEP
26.5 kDa ASTVPLTGVIFEPFE

Fig. 6 (A) Sequence comparisons between the peptides of BSF from the MASCOT program and those from the reported amino acid sequence of SSF (13) and (B) 15 N-terminal sequence residues of two subunits of BSF. Sequence prior to one is the plant specific sequence found in the NH_2 extremity of the mature subunit (extension peptide, EP). Peptides from the PMF of the 28.0 and 26.5 kDa subunits from BSF matched with MASCOT database research are shown below the sequences of SSF subunits. Identified amino acid sequences by MALDI-TOF-MS/MS are underlined. Different amino acid residues between BSF and SSF are shown in bold. Residues in green indicate those that have been suggested to form the deduced ferroxidase centre. N-terminal sequence residues of two subunits are in bold.

subunits (28 and 26.5 kDa) of BSF were determined by automated Edman degradation, which are a part of the EP. The results were shown in Fig. 6B. The N-terminal amino acid sequences of the 28 and 26.5 kDa subunit of BSF are ASNAPAPLAGVIFEP and ASTVPLTGVIFEPFE (Fig. 6B), respectively, which are found in the N-terminal of SSF subunit (Fig. 6A, in bold). All these results indicate that BSF and SSF are very similar in primary structure.

On the other hand, it is observed that the PMF of the 28.0 kDa subunit of BSF is pronouncedly distinct from that of its 26.5 kDa subunit, suggesting that the 26.5 kDa is not produced from the degradation of the 28.5 kDa. Similarly, the PMF of both 28.0 and 26.5 kDa subunits from SSF are different from each other, again suggesting that the two subunits are derived from different precursors. Consistent with present observation, the 28.0 and 26.5 kDa subunits of PSF were reported to be different from one another (*14*). Further support for this conclusion comes from recent studies showing that the two subunits 26.5 kDa (H-1) and 28.0 kDa (H-2) of soybean ferritin are encoded by two genes named SferH-1 and SferH-2 (*13*, *28*). Thus, it seems that phytoferritin from legume seeds are controlled by multiple genes. Indeed, cowpea has at least four different ferritin genes, one that encodes a protein with 97% sequence identity to SSF (*29*).

Comparison of Fe^{2+} oxidative deposition and iron release between BSF and SSF

Although BSF and SSF share high sequence identity, their subunit composition is significantly different (Fig. 3B and Supplementary Fig. 1S). The 26.5 and 28.5 kDa subunit numbers are ~12 and 12 for SSF, and 16 and 8 for BSF, respectively, based on SDS–PAGE analysis. Therefore, it is of special interest to know whether the subunit composition of ferritin has effect on either iron oxidative deposition in ferritin or reductive release from ferritin. First, the kinetics of Fe^{2+} oxidative deposition in the two ferritins was determined on stopped flow in conjunction with UV/vis spectrophotometer by measuring the formation of μ-oxo $diFe^{3+}$ complex(es) at 300 nm as previously described (*14*), and results were shown in Fig. 7. At low iron loading of apoferritin (48 Fe^{2+}/protein shell), the initial rate of BSF ($v_0 = 24 \pm 0.8\,\mu M\,s^{-1}$) is nearly identical to that of SSF ($v_0 = 23 \pm 1.2\,\mu M\,s^{-1}$) within experimental uncertainty (Fig. 7A). It has been established that each H-type subunit contains one ferroxidase centre having two iron binding sites (*1–3*). Thus, added 48 Fe^{2+}/protein shell are fast oxidized at 24 ferroxidase centres located within ferritin. These results suggest that the ferroxidase centres in BSF are very similar to those in SSF. In contrast, when 200 Fe^{2+} were added to apoferritin, the initial rate of BSF ($v_0 = 55 \pm 4.2\,\mu M\,s^{-1}$) is ~1.6-fold larger

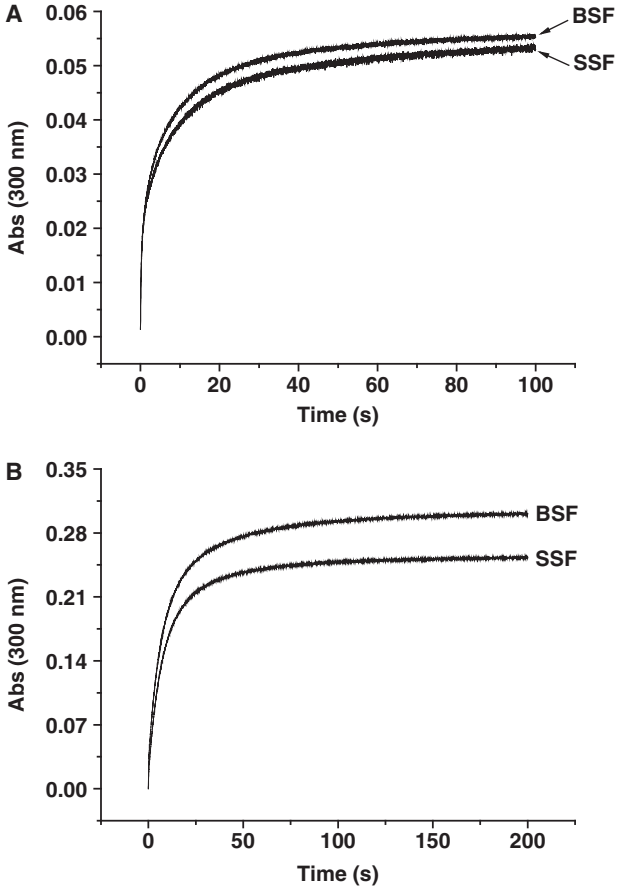

Fig. 7 Kinetic curves of Fe^{2+} oxidation by O_2 in soybean and black bean seed ferritin. Forty-eight Fe^{2+}/apoferritin (A), 200 Fe^{2+}/apoferritin (B). Condition: final [apoferritin] = 0.5 μM, in 0.15 M NaCl and 50 mM Mops pH 7.0, [$FeSO_4$] = 24 μM or 100 μM, 25°C.

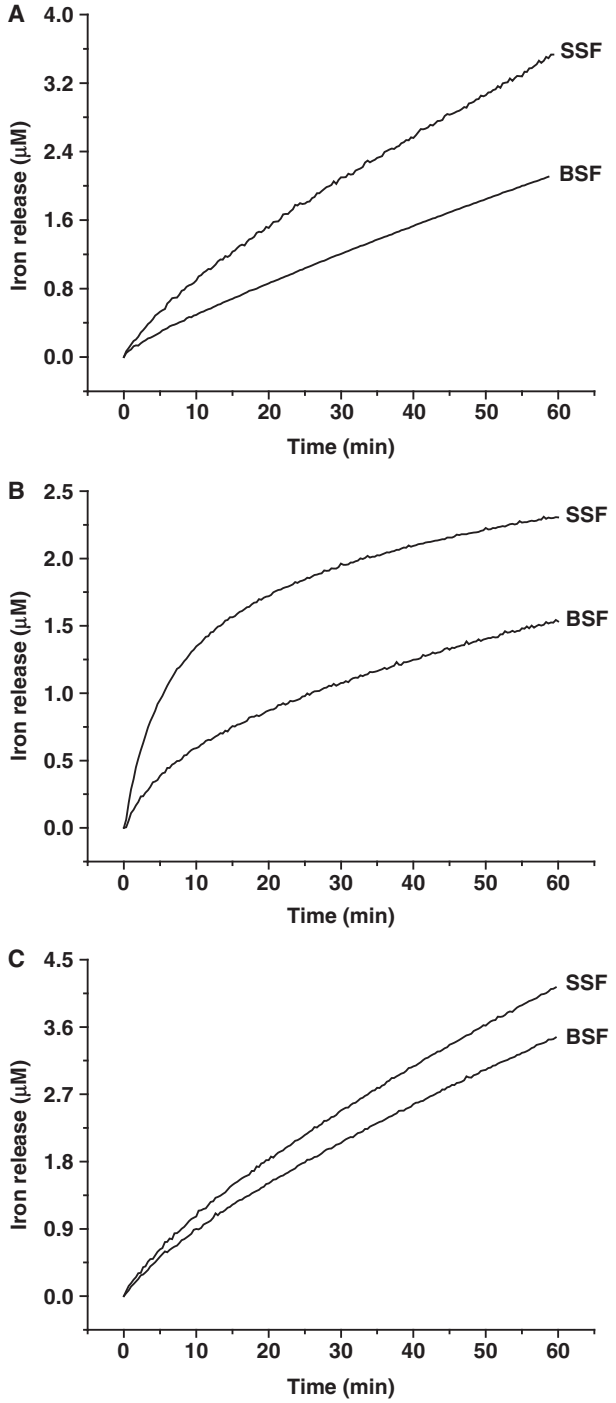

Fig. 8 Kinetic curves of iron release by ascorbate from soybean and black bean seeds ferritin. (A) Native holoferritin, (B) 48 Fe^{3+}/protein, (C) 800 Fe^{3+}/protein. Conditions: 0.2 μM SSF, 1 mM ascorbate, 50 mM Mops, pH 7.0, 0.15 M NaCl, 500 μM ferrozine, 25°C.

than that of SSF ($\nu_0 = 34 \pm 2.4\,\mu M\,s^{-1}$) (Fig. 7B), a result suggesting that the subunit composition has a significant effect on the iron oxidative deposition in ferritin, and the 26.5 kDa subunit is stronger than the 28.0 kDa one in catalysing iron oxidation. Recent studies from our group show that the EP, which usually contains ~30 amino acid residues (*1*, *8*, *13*), located on the exterior surface on the phytoferritin acts as a second ferroxidase centre and is responsible for Fe^{2+} oxidation by O_2 only upon addition of high amount of Fe^{2+} to phytoferritin (>48 Fe^{2+}/shell) (*16*). Since there is high similarity in the primary sequence between PSF and SSF, it is reasonable to believe that the EP from SSF and BSF also has such function. The first 15 amino acid sequence of the 28.0 kDa, ASNAPAPLAGVIFEP is significantly different from that of the 26.5 kDa subunit with sequence ASTVPLTGVIFEPFE (Fig. 6B), so it is likely that the EP of the 26.5 kDa subunit could have a larger catalytic activity than that of its 28.0 kDa counterpart, resulting in a stronger iron oxidative activity of the 26.5 kDa subunit than its analogue upon high iron flux into ferritin. More studies are needed to confirm this idea.

Also, the kinetics of iron release from BSF and SSF was determined spectrophotometrically by measuring the optical density at 562 nm of the ferrozine–Fe^{2+} complex. The results were shown in Fig. 8. It was observed that 1 mM ascorbate significantly induced the iron release from native holoferritin (Fig. 8A), and the initial rate of iron release from BSF ($\nu_0 = 0.011 \pm 0.003\,nM\,s^{-1}$) is approximately two times lower than that from SSF ($\nu_0 = 0.021 \pm 0.005\,nM\,s^{-1}$). Subsequently, holoBSF and holoSSF with different size cores (48 Fe^{3+}/protein

and 800 Fe^{3+}/protein, respectively) were prepared *in vitro* under the same experimental conditions, as previously reported (*23*). Again, similar results were obtained from iron release experiments, namely, iron release from BSF is likewise 1.5–3 times slower than that from SSF (Fig. 8B and C). Since holoBSF and holoSSF have identical core compositions (48 Fe^{3+}/protein or 800 Fe^{3+}/protein), the difference in the iron release most likely comes from their different subunit composition. This result is in accordance with above observation showing that BSF and SSF have different iron oxidative activities at high iron flux into ferritin (Fig. 7B). It has been established that 3- or 4-fold channels in ferritin are the main entrance and exit for iron atoms (*7*, *13*). Unlike the 28.0 kDa subunit, the C-terminal 16 amino acid residues of the 26.5 kDa were cleaved by an unidentified mechanism (*13*), which corresponds to the E-helix of vertebrate ferritin, a short helix forming the narrow channels around the 4-fold intersubunit interaction axes (*13*). Our results are consistent with partial degradation. It was reported that the diameter of this channel is ~1.5 Å in the case of amphibian red cell L-chain ferritin, while that of the 3-fold channel is ~3.7 Å at its narrowest point (*2*). Since BSF contains more 26.5 kDa subunits than does SSF, so it is possible that the pore size of the channel around the 4-fold axes in the BSF is wider than that in SSF, consequently leading to a faster iron release from BSF than SSF (Fig. 8).

In conclusion, this work reports new phytoferritin purified from black bean seed for the first time. This protein shares very high amino acid sequence identity with well-known SSF, but its subunit composition is clearly different from that of SSF. Consistent with their difference in the subunit composition, the activity of the iron uptake and release between the two proteins is also different, indicating that H-1 and H-2 have different activities in the iron uptake and release, which may be related to iron control by phytoferritin.

Supplementary Data

Supplementary Data are available at *JB* Online.

Acknowledgements

National Natural Science Foundation of China (30972045), China High-Tech (863) project (2007AA10Z311) and the Key Laboratory Open Fund of Soybean Biology of Education Ministry.

Conflict of Interest
None declared.

References

1. Liu, X., and Theil, E.C. (2005) Ferritins: dynamic management of biological iron and oxygen chemistry. *Acc. Chem. Res.* **38**, 167–175
2. Harrison, P.M., and Arosio, P. (1996) The ferritins: molecular properties, iron storage function and cellular regulation. *Biochim. Biophys. Acta Bio-Energ.* **1275**, 161–203
3. Chasteen, N.D., and Harrison, P.M. (1999) Mineralization in ferritin: an efficient means of iron storage. *J. Struct. Biol.* **126**, 182–194
4. Arosio, P., Adelman, T.G., and Drysdale, J.W. (1978) On ferritin heterogeneity: further evidence for heteropolymers. *J. Biol. Chem.* **253**, 4451–4458
5. Toussaint, L., Bertrand, L., Hue, L., Crichton, R.R., and Declercq, J.P. (2007) High-resolution X-ray structures of human apoferritin H-chain mutants correlated with their activity and metal-binding sites. *J. Mol. Biol.* **365**, 440–452
6. Bou-Abdallah, F., Zhao, G., Biasiotto, G., Poli, M., Arosio, P., and Chasteen, N.D. (2008) Facilitated diffusion of iron(II) and dioxygen substrates into human H-chain ferritin. A fluorescence and absorbance study employing the ferroxidase center substitution Y34W. *J. Am. Chem. Soc.* **130**, 17801–17811
7. Crichton, R.R., Herbas, A., Chavez-Alba, O., and Roland, F. (1996) Identification of catalytic residues involved in iron uptake by L-chain ferritins. *J. Biol. Inorg. Chem.* **1**, 567–574
8. Lobréaux, S., Yewdall, S.J., Briat, J.F., and Harrison, P.M. (1992) Amino-acid sequence and predicted three-dimensional structure of pea seed (*Pisum sativum*) ferritin. *Biochem. J.* **288**, 931–939
9. Proudhon, D., Wei, J., Briat, J.F., and Theil, E.C. (1996) Ferritin gene organization: differences between plants and animals. *J. Mol. Evol.* **42**, 325–336
10. Waldo, G.S., Wright, E., Wang, Z.H., Briat, J.F., Theil, E.C., and Sayers, D.E. (1995) Formation of the ferritin iron mineral occurs in plastids. *Plant Physiol.* **109**, 797–802
11. Hentze, M.W., and Kuhn, L.C. (1996) Molecular control of vertebrate iron metabolism: mRNA-based regulatory circuits operated by iron nitric oxide and oxidative stress. *Proc. Natl Acad. Sci. USA* **93**, 8175–8182
12. Lescure, A.M., Proudhon, D., Pesey, H., Ragland, M., Theil, E.C., and Briat, J.F. (1991) Ferritin gene transcription is regulated by iron in soybean cell cultures. *Proc. Natl Acad. Sci. USA* **88**, 8222–8226
13. Masuda, T., Goto, F., and Yoshihara, T. (2001) A novel plant ferritin subunit from soybean that is related to a mechanism in iron release. *J. Biol. Chem.* **276**, 19575–19579
14. Li, C., Hu, X., and Zhao, G. (2009) Two different H-type subunits from pea seed (*Pisum sativum*) ferritin that are responsible for fast Fe (II) oxidation. *Biochimie* **91**, 230–239
15. Ragland, M., Briat, J.F., Gagnon, J., Laulhere, J.P., Massenet, O., and Theil, E.C. (1990) Evidence for conservation of ferritin sequences among plants and animals and for a transit peptide in soybean. *J. Biol. Chem.* **265**, 18339–18344
16. Li, C., Fu, X., Qi, X., Hu, X., Chasteen, N.D., and Zhao, G. (2009) Protein association and dissociation regulated by ferric iron, a novel pathway for oxidative deposition of iron in pea seed ferritin. *J. Biol. Chem.* **284**, 16743–16751
17. Laulhere, J.P., Laboure, A.M., and Briat, J.F. (1989) Mechanism of the transition from plant ferritin to phytosiderin. *J. Biol. Chem.* **264**, 3629–3635
18. Lobréaux, S., and Briat, J.F. (1991) Ferritin accumulation and degradation in different organs of pea (*Pisum sativum*) during development. *Biochem. J.* **274**, 601–606
19. Choung, M.G., Baek, I.Y., Kang, S.T., Han, W.Y., Shin, D.C., Moon, H.P., and Kang, K.H. (2001) Isolation and

determination of anthocyanins in seed coats of black soybean (*Glycine max* (L.) Merr.). *J. Agric. Food Chem.* **49**, 5848–5851
20. Treffry, A., Hirzmann, J., Yewdall, S.J., and Harrison, P.M. (1992) Mechanism of catalysis of Fe(II) oxidation by ferritin H chains. *FEBS Lett.* **302**, 108–112
21. Bauminger, E.R., Harrison, P.M., Hechel, D., Nowik, I., and Treffry, A. (1991) Mössbauer spectroscopic investigation of structure-function realations in ferritins. *Biochim. Biophys. Acta* **1118**, 48–58
22. Lowry, O.H., Rosebrough, N.J., Farr, A.L., and Randall, R.J. (1951) Protein measurement with the Folin-Phenol reagents. *J. Biol. Chem.* **193**, 265–275
23. Lee, J., Chasteen, N.D., Zhao, G., Papaefthymiou, G.C., and Gorun, S.M. (2002) Deuterium structural effects in inorganic and bioinorganic aggregates. *J. Am. Chem. Soc.* **124**, 3042–3049
24. Leammli, U.K. (1970) Cleavage of structural proteins during the assembly of the head of bacteriophage T4. *Nature* **227**, 680–685
25. Zhao, G., Bou-Abdallah, F., Arosio, P., Levi, S., Janus-Chandler, C., and Chasteen, N.D. (2003) Multiple pathways for mineral core formation in mammalian apoferritin. The role of hydrogen peroxide. *Biochemistry* **42**, 3142–3150
26. Hynes, M.J., and Coinceanainn, M.Ó. (2002) Investigation of the release of iron from ferritin by naturally occurring antioxidants. *J. Inorg. Biochem.* **90**, 18–21
27. Sczekan, S.R., and Joshi, J.G. (1987) Isolation and characterization of ferritin from soyabeans (*Glycine max*). *J. Biol. Chem.* **262**, 13780–13788
28. Masuda, T., Goto, F., Yoshihara, T., Ezure, T., Takashi, S., Kobayashi, S., Shikata, M., and Utsumi, S. (2007) Construction of homo- and heteropolymers of plant ferritin subunits using an *in vitro* protein expression system. *Protein Expres. Purif.* **56**, 237–246
29. Lescure, A.M., Proudhon, D., Pesey, H., Ragland, M., Theil, E.C., and Briat, J.F. (1991) Ferritin gene transcription is regulated by iron in soybean cell cultures. *Proc. Natl Acad. Sci. USA* **88**, 8222–8226